Clayden, N. J., & Williams, R. J. P. (1982) *J. Magn. Reson. 49*, 383-396.
Clore, G. M., Appella, E., Yamada, M., Matsushima, J., & Gronenborn, A. M. (1989) *J. Biol. Chem. 264*, 18907-18911.
Dalgarno, D. C., Levine, B. A., & Williams, R. J. P. (1983) *Biosci. Rep. 3*, 443-452.
Driscoll, P. C., Hill, A. O., & Redfield, C. (1987) *Eur. J. Biochem. 170*, 279-292.
Dyson, H. J., Holmgren, A., & Wright, P. E. (1989) *Biochemistry 28*, 7074-7087.
Ikura, M., Kay, L. E., & Bax, A. (1990) *Biochemistry 29*, 4659-4667.
Labhardt, A. M., Hunziker-Kwik, E. H., & Wüthrich, K. (1988) *Eur. J. Biochem. 177*, 295-305.
Markley, J. L., Meadows, D. H., & Jardetzky, O. (1967) *J. Mol. Biol. 27*, 25-35.
Pastore, A., & Saudek, V. (1990) *J. Magn. Reson. 90*, 165-176.
Sternlicht, H., & Wilson, D. (1967) *Biochemistry 6*, 2881-2892.
Szilagyi, L., & Jardetzky, O. (1989) *J. Magn. Reson. 83*, 441-449.
Wagner, G., Braun, W., Havel, T. E., Shaumann, T., Go, N., & Wüthrich, K. (1987) *J. Mol. Biol. 196*, 611-639.
Wishart, D. S., Sykes, B. D., & Richards, F. M. (1991) *J. Mol. Biol.* (in press).
Wittekind, M., Reizer, J., & Klevit, R. E. (1990) *Biochemistry 29*, 7191-7200.
Wüthrich, K. (1986) *NMR of Proteins and Nucleic Acids*, Wiley, New York.
Zarbock, J., Clore, G. M., & Gronenborn, A. M. (1986) *Proc. Natl. Acad. Sci. U.S.A. 83*, 7628-7632.
Zuiderwig, E. R. P., Kaptein, R., & Wüthrich, K. (1983) *Eur. J. Biochem. 137*, 279-292.
Zuiderwig, E. R. P., Millison, K. W., Henkin, J., & Carter, G. W. (1988) *Biochemistry 27*, 3568-3580.

Proton Nuclear Overhauser Effect Study of the Heme Active Site Structure of Chloroperoxidase†

L. B. Dugad, X. Wang, C.-C. Wang, G. S. Lukat, and H. M. Goff*
Department of Chemistry, University of Iowa, Iowa City, Iowa 52242
Received July 2, 1991; Revised Manuscript Received October 23, 1991

ABSTRACT: Chloroperoxidase, a glycoprotein from the mold *Caldariomyces fumago*, has been investigated in its ferric low-spin cyanide-ligated form through use of nuclear Overhauser effect (NOE) spectroscopy to provide information on the heme pocket electronic/molecular structure. Spin-lattice relaxation times for the hyperfine-shifted heme resonances were found to be three times less than those in horseradish peroxidase. This must reflect a slower electronic relaxation rate for chloroperoxidase than for horseradish peroxidase as a consequence of axial ligation of cysteine in the former versus histidine in the latter enzyme. Isoenzymes A_1 and A_2 of chloroperoxidase show the largest chemical shift differences near the heme propionate on the basis of NOE measurements. This suggests that the primary structure differences for the two isoenzymes are communicated to the heme group through the ring propionate substituents. A downfield peak has been detected in chloroperoxidase with chemical shift, T_1, and line width characteristics similar to those of the Cε-H proton of the distal histidine in horseradish peroxidase. This finding is in agreement with a previous suggestion for a distal histidine residue. The NOE pattern and T_1's of the peaks in the 0.0 to −5.0 ppm upfield region are consistent with the presence of an arginine amino acid residue in the heme pocket near either the 1-CH_3 or 3-CH_3 group. Existence of catalytically important distal histidine and arginine amino acid residues in chloroperoxidase shows it to be structurally similar to peroxidases rather than to the often compared monooxygenase, cytochrome P-450. This result supports the earlier conclusions of Sono et al. [Sono, M., Dawson, J. H., Hall, K., & Hager, L. P. (1986) *Biochemistry 25*, 347-356].

Chloroperoxidase (CPO)[1] has been the subject of several investigations because of its versatile catalytic properties typical of peroxidases, catalases, and oxygenases (Hewson & Hager, 1979; Dawson & Sono, 1987; Dawson, 1988). In addition, CPO catalyzes halogenation (except fluorination) of substrates in the presence of halide ions and hydrogen peroxide (Hager et al., 1966).

Chloroperoxidase is a glycoprotein (42 kDa) with a heme prosthetic group (Figure 1A) secreted by the mold *Caldariomyces fumago* (Morris & Hager, 1966). The axial ligand to the heme iron atom in chloroperoxidase, unlike other known heme peroxidases, is a cysteine sulfur atom (Bangcharoenpaurpong et al., 1986; Blanke & Hager, 1988). Various spectral properties of chloroperoxidase are similar to those of the monooxygenase cytochrome P-450, presumably due to presence of a cysteine axial ligand to the heme in both enzymes (Dawson & Sono, 1987; Dawson, 1988). The high-resolution X-ray crystal structure of cyt P-450cam is available (Poulos

† This work was supported by NIH Grant GM 28831.

[1] Abbreviations: CPO, chloroperoxidase; HRP, horseradish peroxidase; CCP, cytochrome *c* peroxidase; CPOCN, CCPCN, and HRPCN, cyanide-ligated ferric low-spin complexes of CPO, CCP, and HRP, respectively; cyt P-450, cytochrome P-450; NMR, nuclear magnetic resonance; NOE, nuclear Overhauser effect.

0006-2960/92/0431-1651$03.00/0

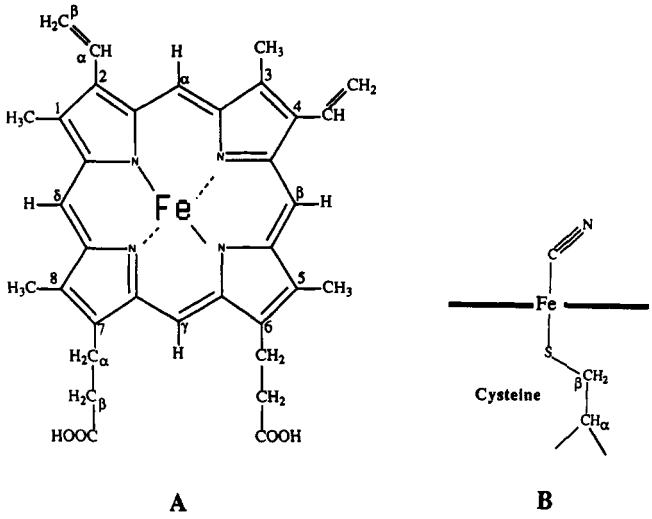

FIGURE 1: Schematic diagram showing (A) the structure of iron protoporphyrin IX and (B) the axial ligands of the heme iron for CPOCN.

et al., 1986). However, little is known about the heme active site environment of chloroperoxidase. Amino acid sequence information is available (Fang et al., 1986), but the three-dimensional structure of the enzyme is undetermined.

The question of structural similarity of chloroperoxidase to other peroxidases or to a monooxygenase has been of some interest (Sono et al., 1986; Dawson & Sono, 1987). Recent work on the ligand-binding properties of chloroperoxidase has suggested the active site structure of chloroperoxidase is like that of peroxidases in spite of its spectroscopic similarity to cyt P-450 (Sono et al., 1986). Due to the unique catalytic behavior of chloroperoxidase, it is of interest to learn how nature has accomplished such a diverse catalytic activity for a single enzyme. The presence of distal histidine and arginine amino acid residues in the heme pocket of peroxidases has been implicated in their catalytic function (Poulos & Kraut, 1980). Evidence for a histidine residue in the heme pocket of chloroperoxidase has recently been obtained by chemical modification experiments (Blanke & Hager, 1990). However, the monooxygenase cyt P-450cam crystal structure data reveal no distal histidine and an arginine amino acid residue placed much farther away from the heme (Poulos et al., 1986). Thus, the active site structural differences are clearly apparent for peroxidase versus monooxygenase enzymes.

Use of NMR spectroscopy for the paramagnetic ligated forms of chloroperoxidase has provided some insight into its active site structure (Goff et al., 1985; Lukat & Goff, 1986, 1990). Comparison of proton NMR spectral characteristics of chloroperoxidase with well-characterized enzymes such as horseradish peroxidase (Thanabal et al., 1987a,b, 1988) and cytochrome *c* peroxidase (Satterlee & Erman, 1991) should lead to more detailed information about the heme environment of the *Caldariomyces* enzyme. In this paper, we report an NOE study on the cyanide-ligated complex (Figure 1B) of chloroperoxidase to obtain electronic and molecular structural information about the heme active site.

Materials and Methods

Chloroperoxidase was isolated from the growth medium of the mold *C. fumago* according to the previously reported method (Gonzalez-Vergara et al., 1985). The protein preparations contained two isoenzymes A_1 and A_2 in agreement with the earlier report (Goff et al., 1985). All protein preparations showed an R_z value of 1.4. Samples for NMR

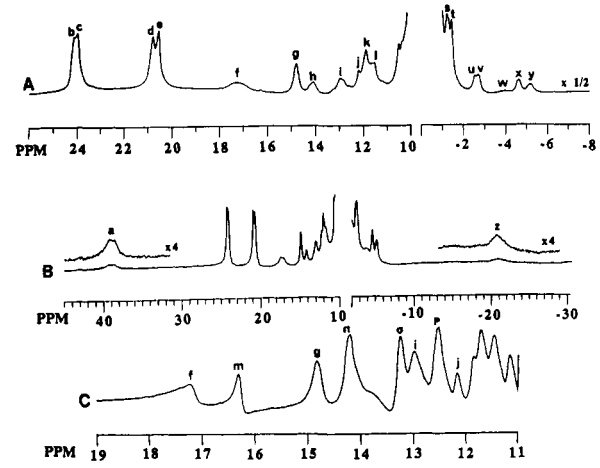

FIGURE 2: (A) 600-MHz proton NMR spectrum of the ferric low-spin cyanide complex of chloroperoxidase in D_2O and 10 mM phosphate buffer, pH 6.0, at 298 K showing the paramagnetically shifted peaks. (B) Spectrum of the same sample as in panel A recorded with a repetition rate of 100 s^{-1} to observe the fast relaxing peaks a and z. (C) Downfield spectral region of CPOCN in 90% H_2O/10% D_2O recorded with the Redfield selective excitation pulse sequence.

spectroscopy were prepared by repetitive (>6) isotope exchange of protein solution in H_2O with D_2O. Protein concentrations were 2 mM in 0.5 mL of D_2O when transferred to a 5-mm NMR tube. Samples contained 10 mM phosphate buffer at pH 6.0. The cyanide complex of native CPO was formed by addition of a 10-fold excess potassium cyanide.

Proton NMR spectra were recorded on a Bruker AMX-600 spectrometer at 600.14 MHz. The NOE experiments were performed by collection of free induction decays with on- and off-resonance irradiation in the interleaved mode. The resonance of interest was irradiated with weak decoupler power (<0.5 W), and a repetition time of 0.5 s was used to obtain the steady-state NOEs. The NOE experiments were repeated at various decoupler power and reference frequencies in order to differentiate between off-resonance effects and NOE. Spin–lattice relaxation times of paramagnetically shifted resonances were measured by the standard inversion–recovery pulse sequence with a repetition rate of 1 s^{-1} and a 90° observe pulse of 9 μs. The T_1 values were estimated from the null point by the relation $T_1 = \tau/\ln 2$. The NOE (steady-state) and T_1 data were analyzed to obtain the interproton and iron–proton distances with the standard equations as described elsewhere (Noggle & Schirmer, 1971; Neuhaus & Williamson, 1988; Thanabal et al., 1987a,b). Steady-state NOE enhancement between two protons *i* and *j* is defined for the present study by $(I_i^\circ - I_i)/I_i^\circ$. Chemical shifts are reported in parts per million and referenced with respect to the residual HOD signal, which in turn was calibrated with 2,2-dimethyl-2-silapentane-5-sulfonate (DSS). Spectra in H_2O solution were acquired by the Redfield selective excitation pulse sequence (Redfield et al., 1975) with the carrier frequency placed near the region of interest.

Proton NMR spectra of the ferric low-spin form were obtained with a 30- or 45-kHz sweep-width, 8192 data points, and a repetition time of 0.5 s. Generally, 2000–3000 scans were accumulated, and the resulting FIDs were multiplied by 20-Hz exponential apodization.

Results

The proton NMR spectrum of the ferric low-spin CPOCN complex in D_2O is shown in Figure 2A. The spectrum is equivalent to that reported earlier (Goff et al., 1985), except that the ratio of isoenzymes A_1 and A_2 is nearly 1:1 in the

Table I: Proton NMR Parameters of Paramagnetically Shifted Resonances in CPOCN at 298 K, in 10 mM Phosphate Buffer, pH 6.0

peak	chemical shift (ppm) (intensity)	T_1 (ms)[a]	assignment
a	38.6	1.5	Cys β-CH
b	24.1 (3)	33	5-CH_3 or 8-CH_3
c	24.0 (3)	35	5-CH_3 or 8-CH_3
d	20.8 (3)	30	1-CH_3 or 3-CH_3
e	20.6 (3)	34	1-CH_3 or 3-CH_3
f	17.3 (2)	6	
m[b]	16.3	200	
g	14.8 (2)	29	
n[b]	14.2	160	
h	14.1 (1)	35	propionate α-CH
o[b]	13.3	220	
i	13.0 (2)	35	propionate α-CH
p[b]	12.6	175	
j	12.2 (1)	220	His Cϵ-H ?
k	11.9 (2)	28	
l	11.6 (1)	30	propionate α-CH
s	−1.2	c	
t	−1.4	c	Arg $-CH_2$?
u	−2.5 (1)	70	Arg $-CH_2$?
v	−2.7 (2)	75	Arg $-CH_2$?
w	−3.9 (1)	7	
x	−4.6 (2)	80	Arg $-CH_2$?
y	−5.1 (2)	58	Arg $-CH_2$?
z	−20.6	1.5	Cys β-CH

[a] Reported T_1 values have ±10% error with the exception of signals a and z, which have ±25% error. [b] Labile proton resonances. [c] Not determined.

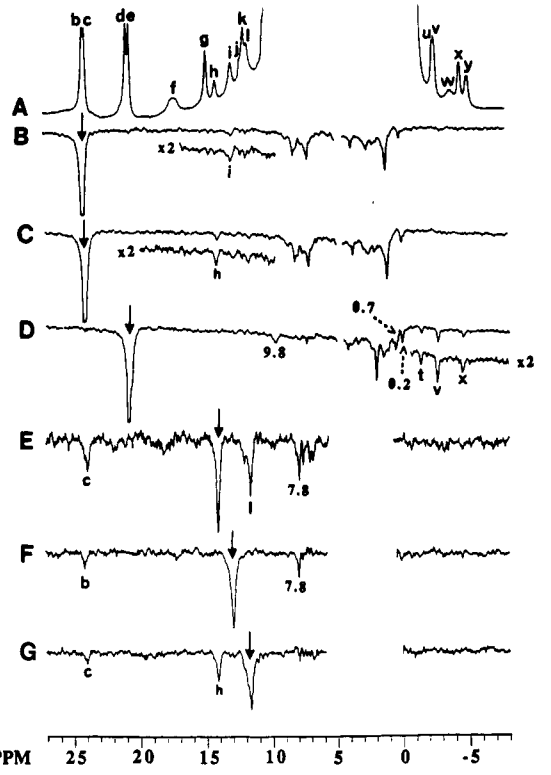

FIGURE 3: (A) 600-MHz proton NMR reference spectrum of 2 mM CPOCN in D_2O, 10 mM phosphate buffer, pH 6.0, at 298 K; (B–G) NOE difference spectra obtained upon irradiation of peaks b, c, d, h, i, and l, respectively. The irradiated peaks are shown with the downward arrow in each difference spectrum.

current sample preparation. The spectrum collected at a fast repetition rate is included in Figure 2B to show the presence of fast relaxing peaks near 39 (peak a) and −20.6 (peak z) ppm as reported previously (Goff et al., 1985). The spectrum showing the presence of four exchangeable protons in the 12–17 ppm region obtained in 90% H_2O solution is shown in Figure 2C. Chemical shifts and T_1 values of all paramagnetically shifted peaks are reported in Table I along with their relative intensities. Peaks b, c, d, and e (Figure 2A) are of three-proton intensity each and arise from two heme methyl protons of isoenzymes A_1 and A_2. The two isoenzymes show very similar or identical chemical shifts for many hyperfine-shifted resonances. This is clear from the measurement of relative proton intensities of each peak (Table I) and the observed NOE pattern (Figure 3).

The fast relaxing peaks a and z (Figure 2B) are assigned to the β-CH_2 protons of the coordinated cysteine amino acid residue. Peak a consists of separately resolved signals for the A_1 and A_2 isoenzymes. Individual isoenzyme signals are not apparent in peak z, but the non-Lorentzian line shape of this signal implies closely overlapping peaks. Peaks a and z exhibit large contact shift and very efficient relaxation, similar to the proximal histidine ring protons in HRPCN (Thanabal et al., 1987a,b). Assignment of peaks a and z to Cys-CH_2 protons is consistent with relaxation properties and expected distance to the iron center. Assuming only metal-centered relaxation, T_1 is proportional to r^6, where r is the metal–proton distance. Hence, by comparison of a heme methyl T_1 of 33 ms and an iron–methyl distance of 6.0 Å, the approximate 1.5-ms T_1 of peaks a and z should be associated a 3.6-Å metal–proton distance. This value is not unreasonable for Cys-CH_2 protons. Efforts to relate the a and z signals by NOE were unsuccessful due to the short relaxation times.

There are two additional relatively fast relaxing peaks f and w with T_1's of 6–7 ms observed in the spectrum of CPOCN. These peaks likely arise either from the *meso*-protons of the heme or from the α-CH proton of the ligated cysteine amino acid residue, as these are the only remaining residues with metal–proton distance sufficiently short to cause such efficient relaxation.

It is interesting to note that the T_1's of the heme resonances in CPOCN (Table I) are typically three times smaller than those of HRPCN (Thanabal et al., 1988) and *Coprinus macrorhizus* peroxidase (L. B. Dugad and H. M. Goff, unpublished results). Little difference in the T_2 values of these resonances (as measured from line widths) was observed for the three peroxidases. These differences are discussed below in terms of the axial amino acid ligand variation among the peroxidases.

Four exchangeable proton signals with T_1's in the 160–220-ms range (Table I) and chemical shifts in the 12–17 ppm range were observed (peaks m, n, o, and p in Figure 2C). Irradiation of these peaks showed no NOE to signals in the paramagnetic region. The chemical shifts of these exchangeable protons were invariant in the 5–35 °C temperature range. Variable temperature data for the nonexchangeable protons have been reported (Lukat & Goff, 1986).

The NOE difference spectra obtained upon irradiation of several downfield shifted resonances are shown in Figure 3. The reference spectrum of CPOCN is shown in Figure 3A. Irradiation of the heme methyl peaks b and c shows several common NOEs (Figure 3B,C). The heme methyl peak b shows an NOE (−6%) to peak i at 13.0 ppm, whereas peak c shows an NOE (−6%) to peak h at 14.1 ppm. The numbers in parentheses indicate magnitude of the NOE. Irradiation of the heme methyl peaks d (Figure 3D) and e (not shown) gives an identical NOE pattern which is different than the one obtained by irradiation of peaks b and c. Both peaks d and e show NOE to three upfield-shifted peaks t (−3.5%), v (−9%), and x (−5%) (Figure 3D). In addition, they also show an NOE to peaks at 0.2 (−11%), 0.7 (−16%), and 9.8 (−7%) ppm.

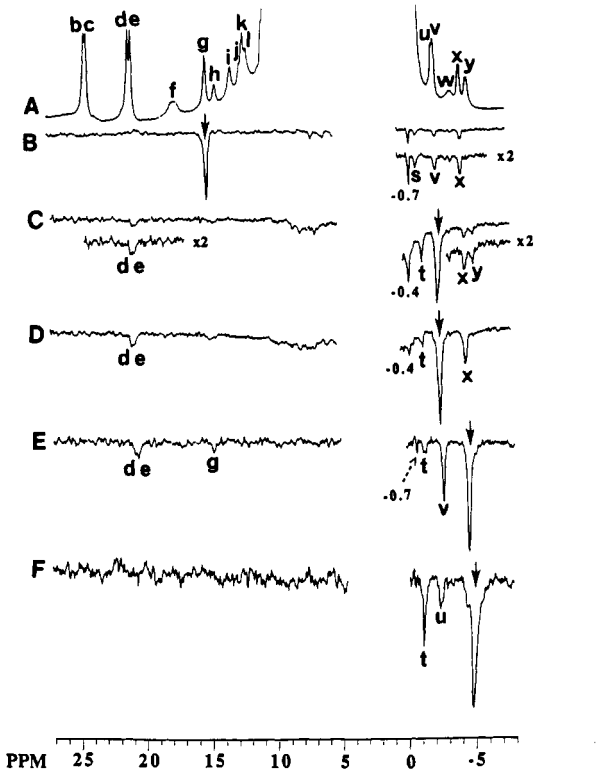

FIGURE 4: (A) 600-MHz proton NMR reference spectrum of 2 mM CPOCN in D_2O, 10 mM phosphate buffer, pH 6.0, at 298 K; (B–F) NOE difference spectra obtained upon irradiation of respective peaks g, u, v, x, and y, respectively.

Irradiation of peak h shows a reciprocal NOE to peak c (−30%) (Figure 3E) and a large NOE (−60%) to peak l. The NOE is observed from peak i to peak b (−24%) and to a peak at 7.8 (−30%) ppm (Figure 3F). The NOE from peak l to peak h (−50%) and to peak c (−20%) is shown in Figure 3G.

In Figure 4 are shown the NOE difference spectra obtained upon irradiation of the upfield-shifted resonances (peaks u, v, x, and y) in the −2 to −6 ppm region, along with NOE-related downfield peak g. Irradiation of peak g shows NOE connectivity to a peak at −0.7 (−30%) ppm and to peaks s (−15%), v (−13%), and x (−16%) (Figure 4B). Irradiation of peak u gives an NOE to peaks d (−9%), e (−9%), t (−33%), x (−14%), y (−12%), and a −0.4 (−50%) ppm peak shown in Figure 4C. Irradiation of peak v shows an NOE to peaks d (−14%), e (−14%), t (−16%), x (−45%), and a peak at −0.4 (−16%) ppm (Figure 4D). The NOE between peaks v and x is large, indicating that they form a $-CH_2$ pair of protons. Irradiation of peak x shows an NOE to peaks d (−16%), e (−16%), g (−14%), t (−15%), v (−57%), and a peak at −0.7 (−15%) ppm (Figure 4E). Irradiation of peak y shows an NOE to peaks t (−50%) and u (−22%) (Figure 4F). The large NOE observed between peaks t and y is again indicative of protons with spatial proximity as a $-CH_2$ pair.

Discussion

Electronic Structure and Mercaptide Coordination. Observation of much shorter T_1's for the heme resonances in CPOCN (Table I) as compared to HRPCN (Thanabal et al., 1987a,b) suggests differences in the electronic relaxation behavior of the two peroxidases. The considerably slower electronic relaxation in CPOCN as evidenced by shorter nuclear T_1 values is also correlated with a somewhat reduced g anisotropy (Hollenberg et al, 1980). Although the net effect of reduced magnetic anisotropy for CPOCN may be smaller dipolar shifts, the perturbation of dipolar shifts for individual signals cannot be predicted without definition of the magnetic axes. The basis for selective modulation of T_1 values presumably is related to cysteine (CPO) versus histidine (HRP) ligation. There are no appropriate model compounds for further evaluation of the phenomenon.

Existence of Isoenzymes. The present NOE results confirm the earlier conclusion (Goff et al., 1985) that multiple heme methyl signals are due to the presence of isoenzymes and are not the result of heme disorder. Very similar (or identical) NOE connectivities for sets of heme methyl signals (b, c and d, e) in CPOCN are only consistent with a common protein environment for a given set of heme methyl residues. Heme disorder would place a given methyl group in different protein environments, and hence the NOE patterns for a set of signals would differ.

Assignment of Resonances. The two methyl peaks b and c show NOE (Figure 3) to a peak (peak b to peak i, and peak c to peak h) that has a geminal partner (see below). This type of NOE pattern is observed for the heme methyl group near the propionate (Figure 1A) substituent (Thanabal et al., 1987a,b). Therefore, the two heme methyl peaks b and c of the two isoenzymes can be assigned to either the 5-CH_3 or 8-CH_3 group. The other two heme methyl peaks d and e are then assigned to either 1-CH_3 or 3-CH_3 groups, on the basis of their NOE pattern, which is different than that of methyls b and c. Methyl peaks d and e show an NOE to two peaks at 0.2 and 0.7 ppm that are tentatively assigned as β-CH_2 protons of the 2-vinyl or 4-vinyl (Figure 1A) substituent on the basis of NOE magnitude and pattern. Vinyl β-CH_2 proton signals are observed for *C. macrorhizus* peroxidase near 0.0 ppm (L. B. Dugad and H. M. Goff, unpublished results) rather than in the −3 to −5 ppm region. The NOEs observed in the diamagnetic region from irradiation of any of the paramagnetically shifted peaks cannot be definitively assigned at present in the absence of crystal structure information.

Peaks h and i are assigned to either a 6-α-H or 7-α-H propionate proton of separate isoenzymes. Thus, the large NOE between peaks h and l implies a geminal pair of α-CH_2 protons. Isoenzymes A_1 and A_2 generally exhibit very similar chemical shift values. For example, the two resolved heme methyl signals show differences of only 0.1 and 0.2 ppm for the two isoenzymes. However, signals h and i, assigned to α-CH propionate protons in the two isoenzymes, are separated by 1.1 ppm. It thus appears that the protein modification that defines isoenzymes A_1 and A_2 is either located in the vicinity of the heme propionate or is communicated to the heme via the propionate side chain. (Note that a 0.8 ppm difference between the two isoenzymes is seen in peak a, but this shift out of a 35 ppm hyperfine shift is relatively much smaller than the difference observed for the propionate signals.)

Peak j with a T_1 of 220 ms is the only peak in the downfield region with such a large T_1 value. This peak in D_2O solution shows no NOE to any other resolved peak. The chemical shift, T_1, and NOE pattern of this peak are very similar to those of the previously identified distal histidine Cϵ-H proton in HRPCN and CCPCN (Thanabal et al., 1988; Satterlee & Erman, 1991) and in the *C. macrorhizus* peroxidase cyanide complex (L. B. Dugad and H. M. Goff, unpublished results). The NOE pattern in H_2O solution for CPOCN, however, is sufficiently different than the one observed for HRPCN to unambiguously assign this proton to the distal histidine proton. If peak j is from a distal histidine Cϵ-H proton, the NOE data in H_2O solution suggest absence of or only weak hydrogen bonding between the bound cyanide ion and the distal histidine Nϵ-H proton.

The NOE pattern for the upfield peaks u, v, x, and y (Figure 4) clearly indicates the presence of three $-CH_2$ groups. Peaks t and y, v and x, and u and a −0.4 ppm peak are identified as three geminal pairs of $-CH_2$ protons on the basis of large respective NOEs. Although β-CH_2 vinyl signals may also appear in the near upfield region, assignment of the upfield peaks t, u, v, x, and y as β-CH_2 vinyl protons appears to be ruled out by virtue of NOE connectivity among the signals. Peak g may represent an α-CH vinyl proton with degenerate chemical shift for both isoenzymes. We considered the possibility that geminal peaks v and x were β-CH_2 vinyl signals, as irradiation of peak g gave an NOE to v and x. Irradiation of both peaks v and x produces the same NOE to methyl peaks d/e, and smaller NOEs to peak g. This common NOE to the methyl peak also rules out peaks v and x as β-CH_2 vinyl signals, as all orientations of the vinyl group will place CH_2 protons at differing distances to the adjacent methyl group. Comparison of chemical shifts, relaxation times, and NOE pattern with that of HRPCN (Thanabal et al., 1988) shows that the t, u, v, x, y, and −0.4 ppm peaks are very similar to the signals assigned to the distal arginine residue in the heme pocket of HRPCN. The amino acid residue responsible for the upfield geminal peaks is close to either the 1-CH_3 or 3-CH_3 group on the basis of NOEs to the methyl peaks d and e. Thus, CPO exhibits stereochemistry at the heme active site differing from HRP and CCP, in that the latter enzymes have a distal arginine residue close to propionate bearing pyrroles. The arginine in CCP is close to the 5-CH_3 group (Poulos & Kraut, 1980; Finzel et al., 1984).

A Peroxidase-Like Active Site? The present results point to structural similarity of the CPO heme pocket to the relatively better characterized peroxidases CCP and HRP, rather than to the monooxygenase cytochrome P-450. The presence of a distal histidine residue is suggested for CPOCN, in agreement with the previous chemical modification work of Blanke and Hager (1990). In terms of hydrogen bonding with the ligated cyanide ion, the distal histidine in CPOCN seems to differ from other peroxidases. The distal histidine Nϵ-H proton is hydrogen bonded to the ligated cyanide ion in HRPCN (Thanabal et al., 1988) and CCPCN (Satterlee & Erman, 1991). There is no distal histidine in the case of cyt P-450cam (Poulos et al., 1986) as shown in the crystal structure.

The presence of an arginine residue in the heme pocket of CPO may be inferred by the current NOE data, although the spatial disposition and heme distance must differ from that in CCP and HRP. The β-CH_2 protons of arginine are 4.5 Å from the heme iron in CCP (Finzel et al., 1984). The arginine in HRP is also placed at a similar distance from the heme as indicated by the T_1 data of the arginine resonances in HRPCN (Thanabal et al., 1988). Calculation of metal–proton distances for CPOCN places the arginine proton peaks t, u, v, x, and y 6.6–6.8 Å from the iron atom. There is no arginine residue close to the heme periphery of cyt P-450. Thus, the active site of CPOCN is qualitatively similar to other peroxidases, although there are subtle differences in terms of the stereochemistry of the two catalytically important distal histidine and arginine amino acid residues. The present NMR results support an earlier prediction of CPO active site structural similarity to the class of peroxidase enzymes (Sono et al., 1986).

References

Bangcharoenpaurpong, O., Champion, P. M., Hall, K. S., & Hager, L. P. (1986) *Biochemistry 25*, 2374–2378.

Blanke, S. R., & Hager, L. P. (1988) *J. Biol. Chem. 263*, 18739–18743.

Blanke, S. R., & Hager, L. P. (1990) *J. Biol. Chem. 265*, 12454–12461.

Dawson, J. H. (1988) *Science 240*, 433–439.

Dawson, J. H., & Sono, M. (1987) *Chem. Rev. 87*, 1255–1276.

Fang, G. H., Kenigsberg, P., Axley, M. J., Nuell, M., & Hager, L. P. (1986) *Nucleic Acids Res. 14*, 8061–8071.

Finzel, B. C., Poulos, T. L., & Kraut, J. (1984) *J. Biol. Chem. 259*, 13027–13036.

Goff, H. M., Gonzalez-Vergara, E., & Bird, M. R. (1985) *Biochemistry 24*, 1007–1013.

Gonzalez-Vergara, E., Ales, D. C., & Goff, H. M. (1985) *Prep. Biochem. 15*, 335–348.

Hager, L. P., Morris, D. R., Brown, F. S., & Eberwein, H. (1966) *J. Biol. Chem. 241*, 1769–1777.

Hewson, W. D., & Hager, L. P. (1979) in *The Porphyrins* (Dolphin, D., Ed.) Vol. VII, part B, pp 295–332, Academic Press, New York.

Hollenberg, P. F., Hager, L. P., Blumberg, W. E., & Peisach, J. (1980) *J. Biol. Chem. 255*, 4801–4807.

Lukat, G. S., & Goff, H. M. (1986) *J. Biol. Chem. 261*, 16528–16534.

Lukat, G. S., & Goff, H. M. (1990) *Biochim. Biophys. Acta 1037*, 351–359.

Morris, D. R., & Hager, L. P. (1966) *J. Biol. Chem. 241*, 1763–1768.

Neuhaus, D., & Williamson, M. P. (1988) *The Nuclear Overhauser Effect in Structural and Conformational Analysis*, Verlag Chemie, New York.

Noggle, J. H., & Schirmer, R. E. (1971) *The Nuclear Overhauser Effect: Chemical Applications*, Academic Press, New York.

Poulos, T. L., & Kraut, J. (1980) *J. Biol. Chem. 255*, 8199–8205.

Poulos, T. L., Finzel, B. C., & Howard, A. J. (1986) *Biochemistry 25*, 5314–5322.

Redfield, A. G., Kunz, S. D., & Ralph, E. K. (1975) *J. Magn. Reson. 19*, 114–117.

Satterlee, J. D., & Erman, J. E. (1991) *Biochemistry 30*, 4398–4405.

Sono, M., Dawson, J. H., Hall, K., & Hager, L. P. (1986) *Biochemistry 25*, 347–356.

Thanabal, V., de Ropp, J. S., & La Mar, G. N. (1987a) *J. Am. Chem. Soc. 109*, 265–272.

Thanabal, V., de Ropp, J. S., & La Mar, G. N. (1987b) *J. Am. Chem. Soc. 109*, 7516–7525.

Thanabal, V., de Ropp, J. S., & La Mar, G. N. (1988) *J. Am. Chem. Soc. 110*, 3027–3035.